

Ab initio Calculations of Intramolecular Exciton Transfer with Reduced Modes in Donor-Bridge-Acceptor Species

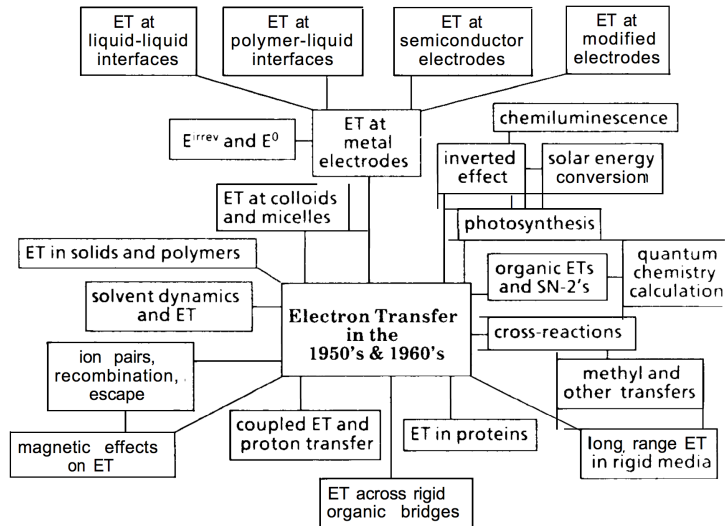
Xunmo Yang

April 20, 2016

Outline

- ▶ Introduction
- ▶ Benchmark of TCLME with Edmiston-Ruedenberg diabatization
- ▶ Primary Mode
- ▶ Application in IR-controlled electron transfer
- ▶ Conclusions

Electron Transfer



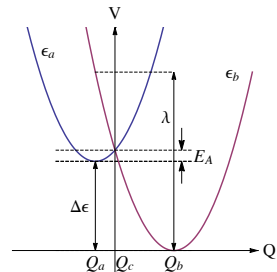
Rudolph A. Marcus - Nobel Lecture: Electron Transfer Reactions in Chemistry: Theory and Experiment".

Marcus Theory

Energy and electronic transport is fundamental in chemistry. The seminal model for calculating transfer rates was developed by Marcus.

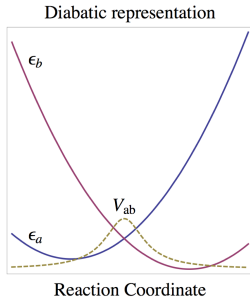
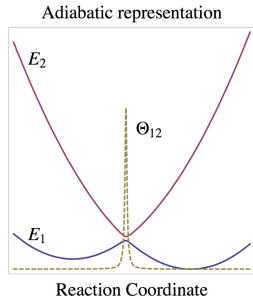
$$H_{dia} = \hat{T}_n + \begin{pmatrix} \epsilon_a(\mathbf{R}) & V_{ab} \\ V_{ab} & \epsilon_b(\mathbf{R}) \end{pmatrix}$$

$$k_{Marcus} = \frac{2\pi}{\hbar} |V_{ab}|^2 \frac{1}{\sqrt{4\pi k_B T \lambda}} e^{-(\lambda + \Delta E)^2 / 4\lambda k_B T}$$



- ▶ Condon approximation: $V_{ab}(\mathbf{R}) = V_{ab}$
- ▶ All vibrations are included in a collective coordinate
- ▶ $k_B T \gg \hbar\omega$

Adiabatic vs. Diabatic Representation



Adiabatic representation

Pros:

- ▶ Eigenstate of electronic Hamiltonian, directly available from quantum chemistry software

Cons:

- ▶ Potential energy surfaces aren't parabolic (avoided crossing)
- ▶ Sharp derivative coupling near avoided crossing (hard to compute)

Diabatization: Boys & Edmiston-Ruedenberg Localization

$$H_{adia} = \begin{pmatrix} E_1(\mathbf{R}) + T_n(\mathbf{R})_{11} & T_n(\mathbf{R})_{12} \\ T_n(\mathbf{R})_{21} & E_2(\mathbf{R}) + T_n(\mathbf{R})_{22} \end{pmatrix}$$

Construct diabatic states to eliminate dynamical coupling,

- ▶ Exact way $\langle \phi_i(\mathbf{r}; \mathbf{R}) | \nabla_{\mathbf{R}} | \phi_j(\mathbf{r}; \mathbf{R}) \rangle = 0$ (expensive & rarely exist)
- ▶ Intuitive way. Transform H_{adia}

$$H_{dia} = U^T H_{adia} U = \begin{pmatrix} \epsilon_a(\mathbf{R}) + T'_n(\mathbf{R})_{11} & V_{ab}(\mathbf{R}) \\ V_{ab}(\mathbf{R}) & \epsilon_b(\mathbf{R}) + T'_n(\mathbf{R})_{22} \end{pmatrix}$$

to maximize/minimize certain physical property

$$f_{Boys} = \sum_{kl}^{N_{states}} (\langle \phi_k | \vec{r} | \phi_k \rangle - \langle \phi_l | \vec{r} | \phi_l \rangle)^2$$

$$f_{ER} = \sum_k^{N_{states}} \iint d\mathbf{r}_1 d\mathbf{r}_2 \frac{\langle \phi_k | \hat{\rho}(r_1) | \phi_k \rangle \langle \phi_k | \hat{\rho}(r_2) | \phi_k \rangle}{\| \mathbf{r}_1 - \mathbf{r}_2 \|}$$

Diabatization: Generalized Mulliken Hush (GMH)

$$\begin{pmatrix} |\phi_a\rangle \\ |\phi_b\rangle \end{pmatrix} = U^T \begin{pmatrix} |\psi_1\rangle \\ |\psi_2\rangle \end{pmatrix} = \begin{pmatrix} \cos\theta & \sin\theta \\ -\sin\theta & \cos\theta \end{pmatrix} \begin{pmatrix} |\psi_1\rangle \\ |\psi_2\rangle \end{pmatrix}$$

Assuming only the direction along $\vec{\mu}_{11} - \vec{\mu}_{22}$ matters, we project all dipole moments onto $\vec{v} = (\vec{\mu}_{11} - \vec{\mu}_{22})/|\vec{\mu}_{11} - \vec{\mu}_{22}|$.

$$\mu_{ab}^\nu = \langle \phi_a | \vec{\mu} | \phi_b \rangle \cdot \vec{v} = \cos 2\theta \vec{\mu}_{12}^\nu - \frac{1}{2} \sin 2\theta |\vec{\mu}_{11} - \vec{\mu}_{22}|$$

Good diabatic states should have $\mu_{ab}^\nu = 0$, this determines θ and gives

$$|H_{AB}| = |\cos 2\theta H_{12} - \frac{1}{2} \sin 2\theta (H_{11} - H_{22})| = \frac{|\mu_{12}^\nu| |H_{11} - H_{22}|}{\sqrt{|\vec{\mu}_{11} - \vec{\mu}_{22}|^2 + 4|\mu_{12}^\nu|^2}}$$

For linear systems, we further assume $|\mu_{12}^\nu| = |\mu_{12}|$.

Time-convolutionless Master Equation (TCLME)

Bittner and Pereversev developed TCLME for Hamiltonian

$$H = \begin{pmatrix} E_a & \\ & E_b \end{pmatrix} + \sum_{ijq} g_{ijq} |\phi_i\rangle\langle\phi_j| q + \sum_q \hbar\omega_q (n + 1/2)$$

To get this desired form, we assume diabatic potentials are the parabolas same as adiabatic potentials, then at Q_b ,

$$H_{dia} = \begin{pmatrix} \epsilon_a & V_{ab} \\ V_{ab} & \epsilon_b \end{pmatrix} + \left(\sum_i g_{22i} q_i \right) + h.o.$$

Diagonalize the electronic part

$$H = U^T H_{dia} U = \begin{pmatrix} E_a & \\ & E_b \end{pmatrix} + \begin{pmatrix} \sin^2 \theta & \frac{1}{2} \sin 2\theta \\ \frac{1}{2} \sin 2\theta & \cos^2 \theta \end{pmatrix} \sum_{i=1}^{NMode} g_{22i} q_i + h.o.$$

Validity of Assumptions

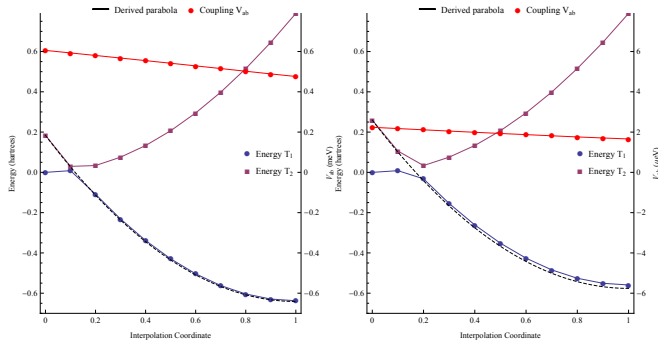


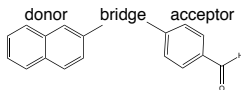
Figure: Adiabatic energy curves and off-diagonal couplings computed along an interpolation coordinate between the $D^* - B - A$ and $D - B - A^*$ equilibrium geometries for (a) c-1,4ee and (b) d-2,6ae.

- ▶ Condon approximation: diabatic couplings are small & steady
- ▶ Parabolic assumption holds well

Benchmark with Closs' Experiments

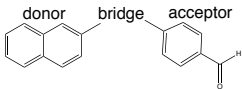
Table: Transfer rates obtained from experiments, TCLME and Marcus theory.

Symbol	Structure	k_{expr} (1/s)	k_{Marcus} (1/s)	k_{TCLME} (1/s)
c-1,3ea		3.3E9	3.9E9	2.2E9
c-1,3ee		7.7E9	2.1E10	2.8E10
c-1,4ea		4.0E7	1.3E7	1.8E7
c-1,4ee		1.3E9	3.9E9	3.6E9
d-2,6ae		1.3E5	1.0E4	4.7E4



Benchmark with Closs' Experiments (Cont'd)

Symbol	Structure	k_{expr} (1/s)	k_{Marcus} (1/s)	k_{TCLME} (1/s)
d-2,6ea		7.0E5	3.9E4	5.8E4
d-2,6ee		3.1E6	5.0E6	4.8E6
d-2,7ae		1.1E7	2.8E7	3.0E7
d-2,7ea		1.5E7	1.8E7	4.3E7
d-2,7ee		9.1E7	3.5E8	3.4E8
M		5.0E10	n.r.	1.2E9



Benchmark with Closs' Experiments (Cont'd)

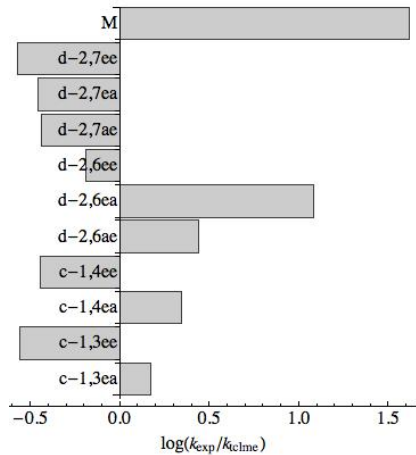


Figure: Comparison between predicted (TCLME) rate constants and the experimental rates. With exception of the methyl bridged and d-2,6ea cases, the TCLME results are in good agreement with the experimental results.

Why TCLME

- ▶ Marcus theory

$$H = \hat{T}_n + \begin{pmatrix} \epsilon_a(\mathbf{R}) & V_{ab} \\ V_{ab} & \epsilon_b(\mathbf{R}) \end{pmatrix}$$

$$k = \frac{2\pi}{\hbar} |V_{ab}|^2 \frac{1}{\sqrt{4\pi k_B T \lambda}} e^{-(\lambda + \Delta E)^2 / 4\lambda k_B T}$$

- ▶ TCLME

$$H = \begin{pmatrix} E_a & \\ & E_b \end{pmatrix} + \sum_{ijq} g_{ijq} |\phi_i\rangle\langle\phi_j| q + \sum_q \hbar\omega_q (n + 1/2)$$

$$H = \begin{pmatrix} E_a & \\ & E_b \end{pmatrix} + \begin{pmatrix} \sin^2 \theta & \frac{1}{2} \sin 2\theta \\ \frac{1}{2} \sin 2\theta & \cos^2 \theta \end{pmatrix} \sum_{i=1}^{NMode} g_{22i} q_i + h.o.$$

TCLME treats normal modes explicitly, which makes projection approach applicable.

Projected Modes

$$H = \begin{pmatrix} E_a & \\ & E_b \end{pmatrix} + \begin{pmatrix} \sum_i g_{11i} q_i & \sum_i g_{12i} q_i \\ \sum_i g_{12i} q_i & \sum_i g_{22i} q_i \end{pmatrix} + \sum_i \frac{p_i^2}{2} + \frac{1}{2} \mathbf{q}^T \Omega \mathbf{q},$$

where

$$\mathbf{q}^T = (q_1, q_2, \dots, q_n), \Omega = \begin{pmatrix} \omega_1^2 & & & \\ & \omega_2^2 & & \\ & & \ddots & \\ & & & \omega_n^2 \end{pmatrix}$$

can be transformed to

$$\Omega' = \begin{pmatrix} \omega_1'^2 & & \gamma_{14} & \cdots & \gamma_{1n} \\ & \omega_2'^2 & \gamma_{24} & \cdots & \gamma_{2n} \\ & & \omega_3'^2 & \gamma_{34} & \cdots & \gamma_{3n} \\ \gamma_{14} & \gamma_{24} & \gamma_{24} & \omega_4'^2 & & \\ \vdots & \vdots & \vdots & & \ddots & \\ \gamma_{1n} & \gamma_{2n} & \gamma_{3n} & & & \omega_n'^2 \end{pmatrix}$$

TCLME Equation

$$\frac{dP_n}{dt} = \sum_{m \neq n} W_{nm}(t) P_m(t) - \sum_{m \neq n} W_{mn}(t) P_n(t)$$

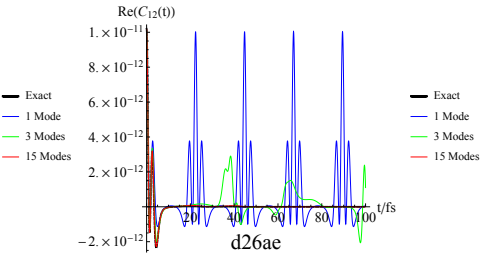
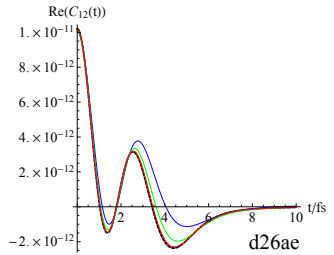
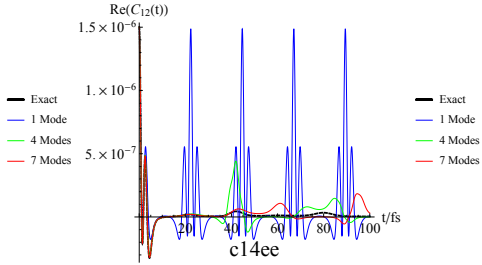
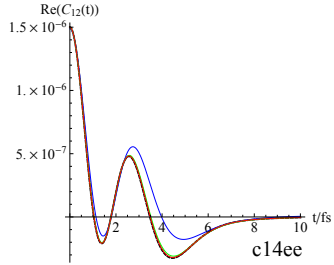
$$W_{nm}(t) = 2\text{Re} \int_0^t d\tau \left\langle \hat{V}_{nm}(0) \hat{V}_{mn}(\tau) \right\rangle e^{-i(\tilde{\epsilon}_m - \tilde{\epsilon}_n)\tau}$$

The renormalization energy is

$$\tilde{\epsilon}_n = \epsilon_n - \sum_i \frac{g_{nni}^2}{\hbar\omega_i}$$

$\left\langle \hat{V}_{nm}(0) \hat{V}_{mn}(\tau) \right\rangle$ is the correlation function.

Projected Modes for c-1,4ee and d-2,6ae



Primary Mode Rate Constant

$$\frac{dP_n}{dt} = \sum_{m \neq n} W_{nm}(t)P_m(t) - \sum_{m \neq n} W_{mn}(t)P_n(t)$$

$$W_{nm}(t) = 2\text{Re} \int_0^t d\tau \left\langle \hat{V}_{nm}(0) \hat{V}_{mn}(\tau) \right\rangle e^{-i(\tilde{\epsilon}_m - \tilde{\epsilon}_n)\tau}$$

$$\tilde{\epsilon}_n = \epsilon_n - \sum_i \frac{g_{nni}^2}{\hbar\omega_i}$$

- ▶ How about using the approximated correlation function and $\Delta\epsilon$ to calculate the rate?
- ▶ How about the approximated correlation function with exact $\Delta\epsilon$?

Primary Mode Rate Constant (Cont'd)

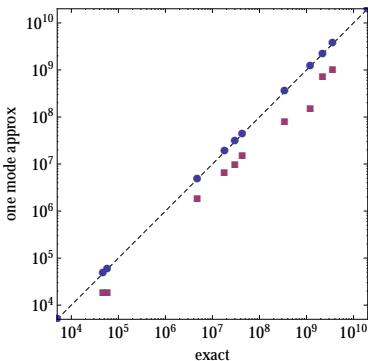


Figure: Comparison between exact rate constant and its primary mode approximation. The blue dots correspond to rates computed using only the primary mode and the renormalized energy for only that mode. The red points use the primary mode and the exact renormalized energies.

Only one mode? Seems easy. Any other way possible?

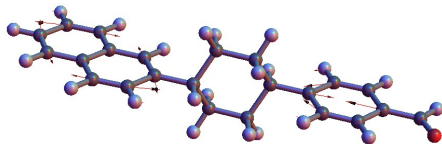
No Normal Mode Works That Well

bridge	ω_1 (eV)	$ g_1 $ (eV)	$ g_{max} $ (eV)
c-1,3ea	0.184	0.367	0.159
c-1,3ee	0.185	0.365	0.162
c-1,4ea	0.185	0.367	0.166
c-1,4ee	0.185	0.370	0.171
d-2,6ae	0.185	0.367	0.159
d-2,6ea	0.185	0.367	0.142
d-2,6ee	0.185	0.365	0.143
d-2,7ae	0.184	0.366	0.165
d-2,7ea	0.185	0.367	0.142
d-2,7ee	0.185	0.370	0.149
M	0.184	0.366	0.160

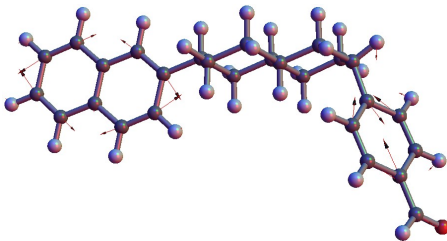
Table: Frequencies and dimensionless electron-phonon couplings for the primary mode. The last column gives the absolute value of the largest coupling constant within the normal mode basis.

$|g_1|$ is more than twice of the largest $|g_i|$. No single normal mod is as representative as the primary mode. Actually, the primary mode generates the largest possible coupling constant.

Primary Mode



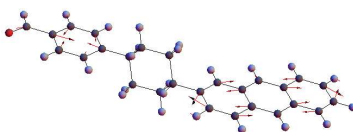
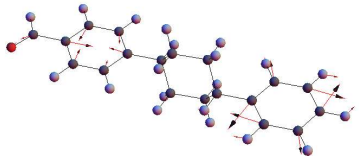
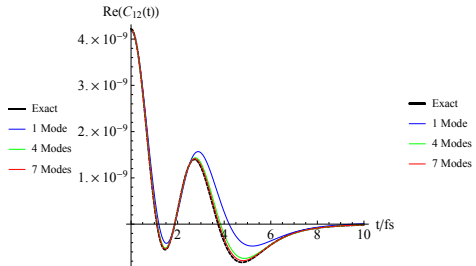
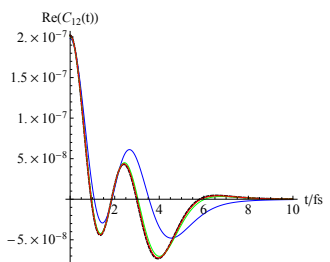
(a) c-1,4ee: $\omega = 1492.47\text{cm}^{-1}$, $g = 0.370\text{eV}$



(b) d-2,6ae $\omega = 1491.09\text{cm}^{-1}$, $g = 0.367\text{eV}$

- ▶ Bridge is barely involved
- ▶ Certain local symmetry

Phenyl and Anthracene as Acceptors



Projection on Moiety

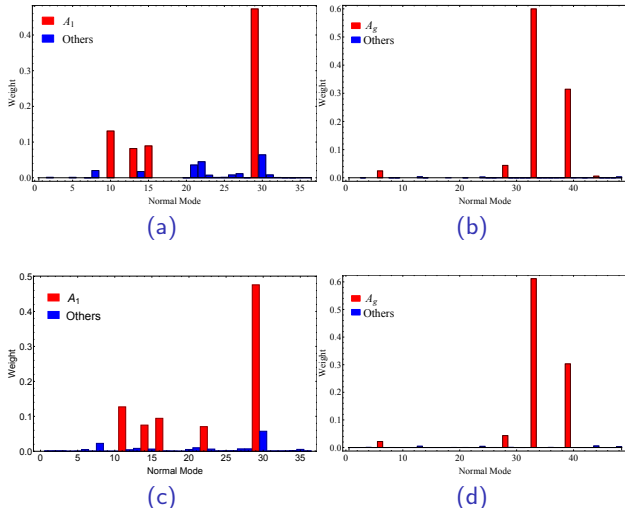


Figure: Projection on (a) benzaldehyde, (b) symmetrized naphthalene in c-1,4ee, (c) benzaldehyde, (d) symmetrized naphthalene in d-2,6ae.

Bridge Is Not Important

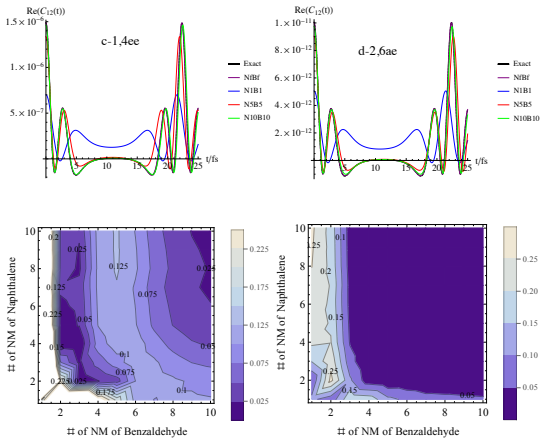
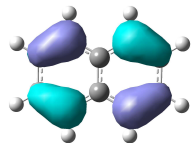
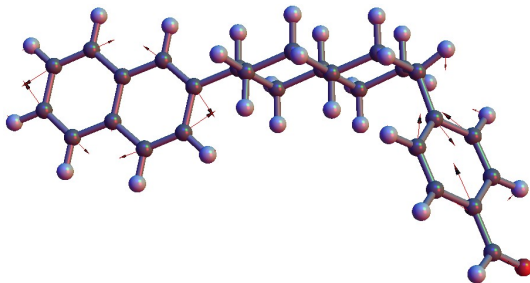
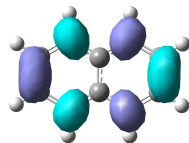


Figure: “Exact” = primary mode. “NfBf” = all normal modes of D and A. “NxBy” = x most significant normal modes on naphthalene + y most significant ones on benzaldehyde. (c) and (d): relative error in rate constants compared to the exact result of c-1,4ee (c) and d-2,6ae (d), respectively.

Primary Mode and Electron Orbital

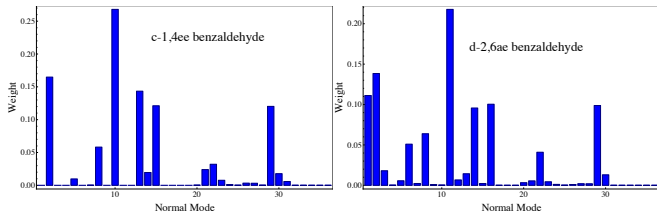


(b) HOMO

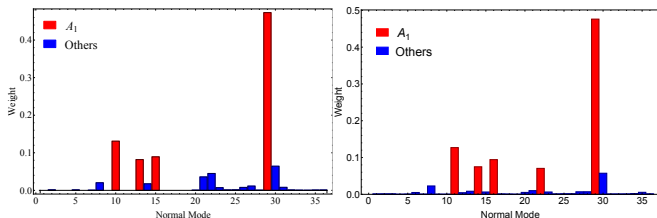


(c) LUMO

Geometry Change On Benzaldehyde

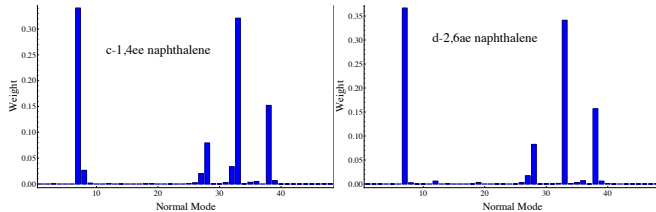


(a) Geometry change

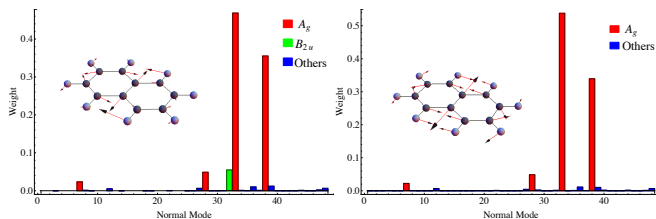


(b) Primary mode

Geometry Change On Naphthalene

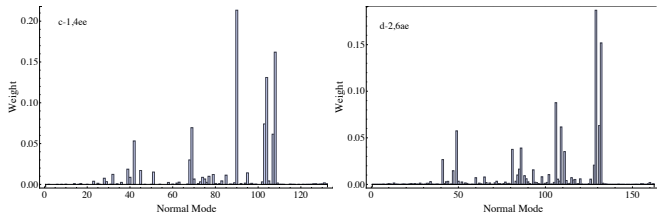


(a) Geometry change

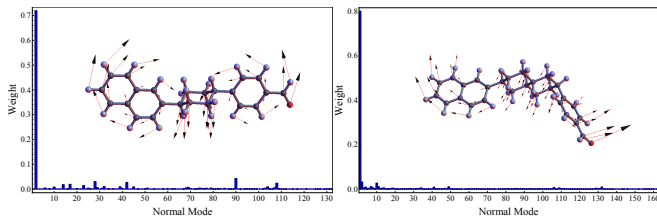


(b) Primary mode

Primary Mode and Geometry Change

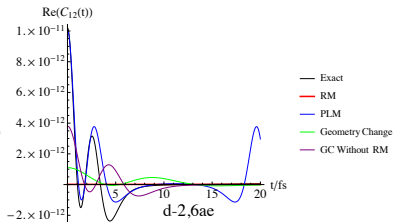
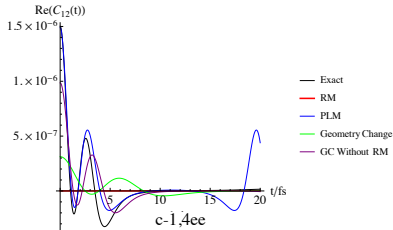
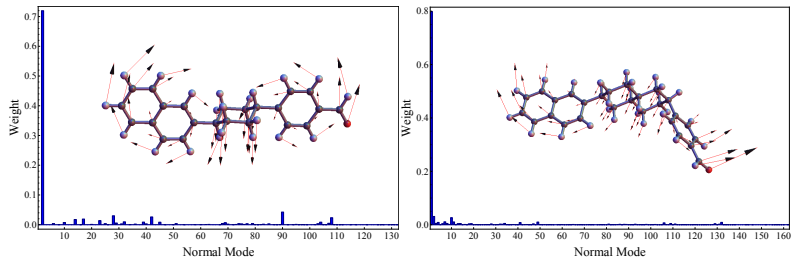


(a) Primary mode



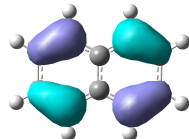
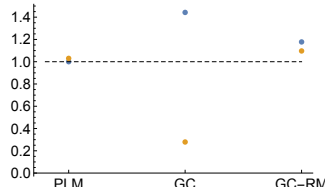
(b) Geometry change

Relaxation Mode Doesn't Contribute to Rate



Internal and Gross Motions

$k_{\text{appr}}/k_{\text{exact}}$



Mode used	Max. bond length difference (\AA)	Max. bond angle difference (rad)
c-1,4ee-PM	0.034	0.053
c-1,4ee-RM	0.160	0.075
d-2,6ae-PM	0.039	0.057
d-2,6ae-RM	0.283	0.135

Table: Approximated geometry using the primary mode (PM) and the relaxation modes (RM) compared to acceptor states

Molecule Structure and Energy Diagram

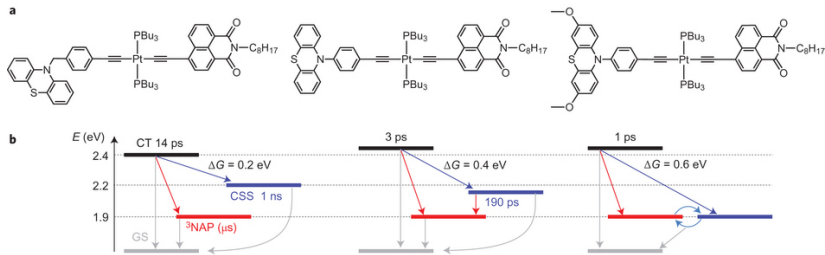
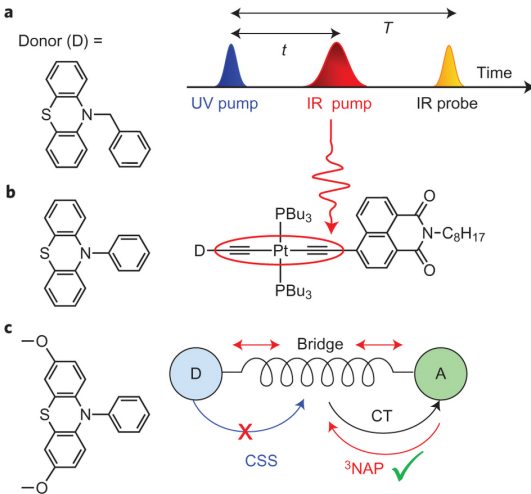


Figure: a. Molecular structure of PTZ-CH₂-Pt-NAP, PTZ-Pt-NAP and OMe-PTZ-Pt-NAP, from left to right (D = PTZ is phenothiazine and A = NAP is naphthalene-monoimide). b. Energy level diagrams for the ET process, with the lifetimes and the driving force (ΔG) of CT \rightarrow CSS transfer indicated.

Delor, Milan, et al. "On the mechanism of vibrational control of light-induced charge transfer in donor–bridge–acceptor assemblies." Nature Chemistry (2015)

IR Control Scheme



Delor, Milan, et al. "On the mechanism of vibrational control of light-induced charge transfer in donor–bridge–acceptor assemblies." Nature Chemistry (2015)

Possible Mechanism

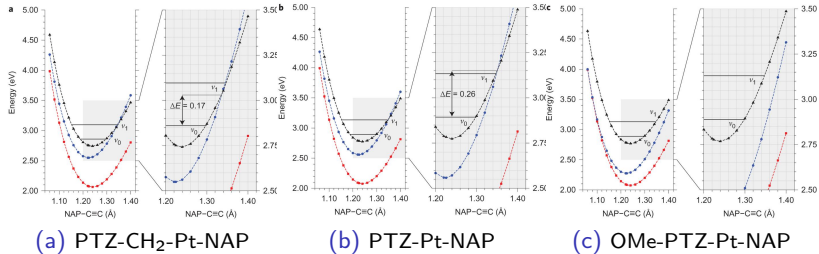


Figure: Calculated energies of the CT (black), CSS (blue) and ³NAP (red) states along the NAP side C≡C coordinate in the ground state geometries, in CH₂Cl₂.

Delor, Milan, et al. "On the mechanism of vibrational control of light-induced charge transfer in donor–bridge–acceptor assemblies." Nature Chemistry (2015)

PTZ-Pt-NAP

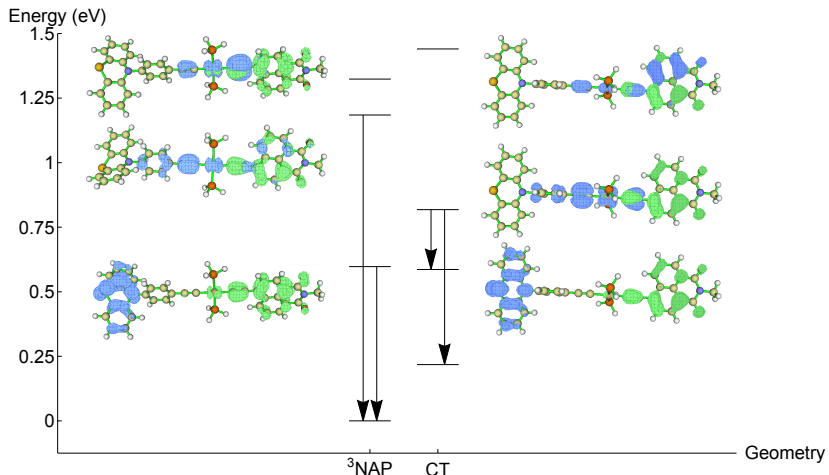
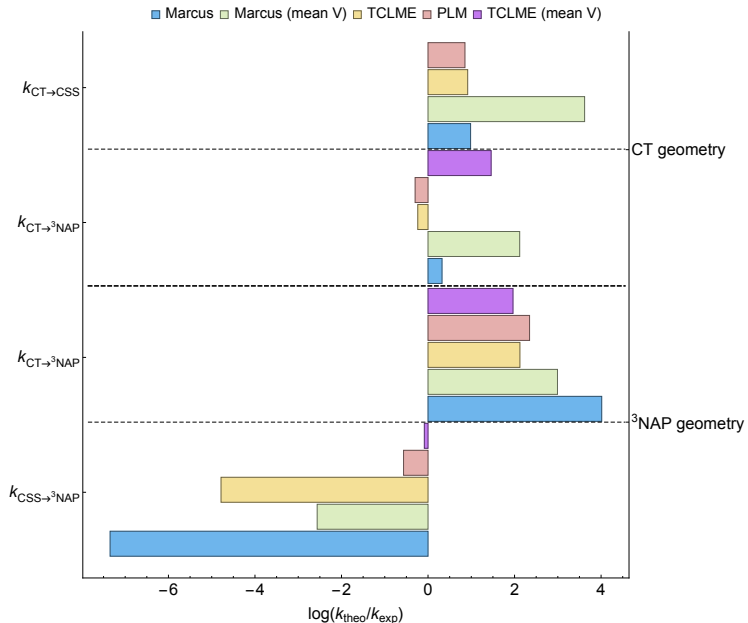
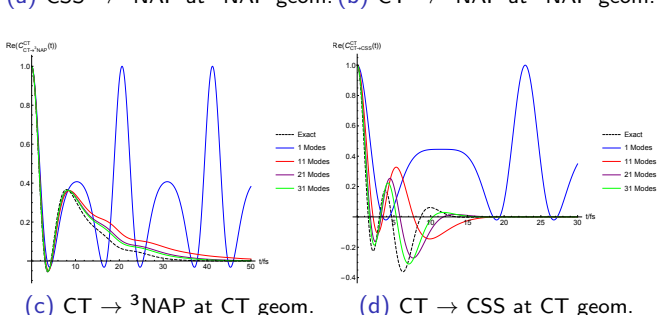
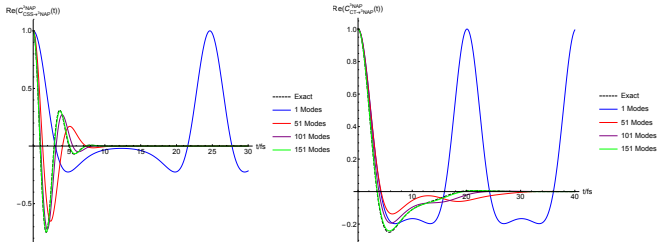


Figure: The energy diagram of triplet states at ${}^3\text{NAP}$ and CT state geometries. The electron/hole distribution are shown as well (green for electron, blue for hole). The arrows indicate the transitions we calculate.

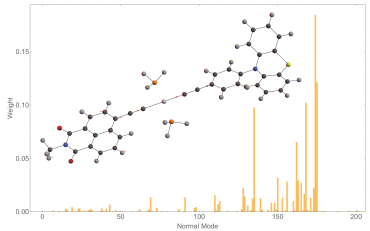
Rate Constants



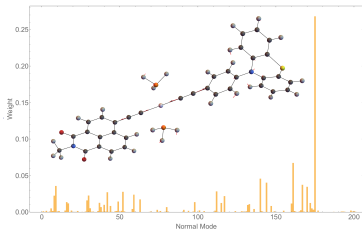
Correlation Functions



Primary Mode



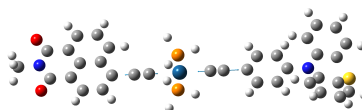
(a) $\text{CT} \rightarrow {}^3\text{NAP}$ at CT geom.



(b) $\text{CT} \rightarrow \text{CSS}$ at CT geom.



(c) 174th mode of CT



(d) 175th mode of CT

Condon Approximation

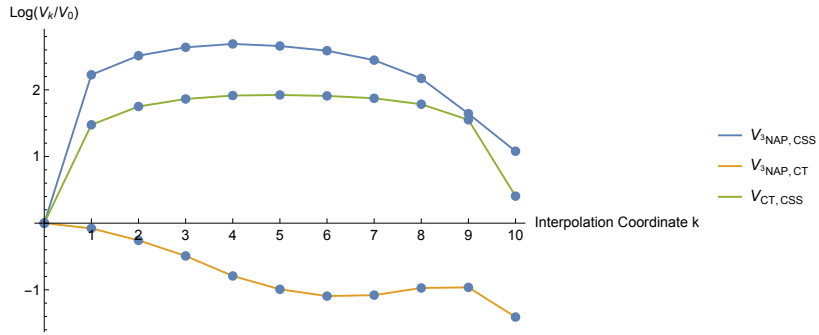
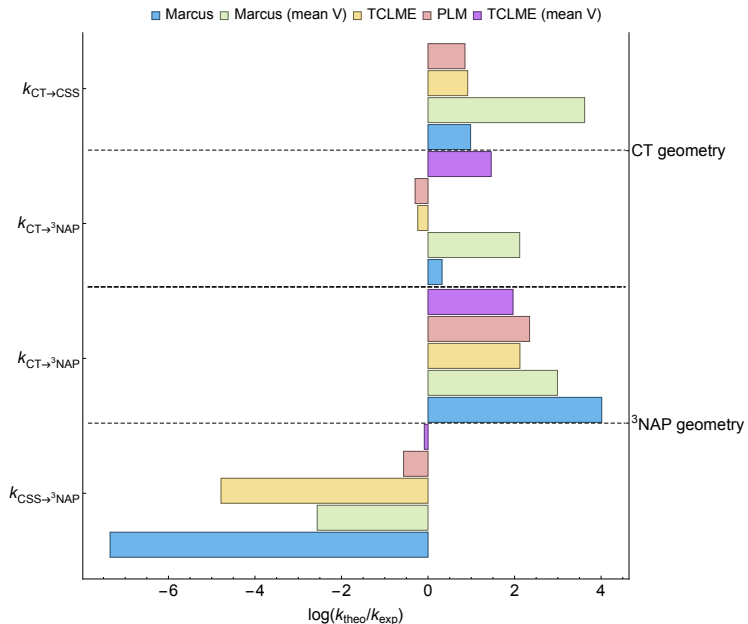


Figure: Diabatic coupling values along the interpolation from the ${}^3\text{NAP} \rightarrow \text{CT}$ geometries. State 0 and 10 stand for the ${}^3\text{NAP}$ and the CT state, respectively.

Rate Constants



Conclusions & Future Work

A general approach for electron energy transfer is developed. It

- ▶ agrees with experiments and previous theoretical studies
- ▶ treats normal modes explicitly, which enables us to analyze them in detail

In the future, we will

- ▶ investigate the regime where Condon approximation fails and how to correct
- ▶ apply it to more complicated system
- ▶ help to design IR-controllable molecules